A Molecular Beam Fourier Transform Microwave Spectrometer in the Range 26.5 to 40 GHz. Tests of Performance and Analysis of the D- and ^{14}N-Hyperfine Structure of Methylcyanide-d_1

I. Merke, W. Stahl, and H. Dreizler

Abteilung Chemische Physik im Institut für Physikalische Chemie der Christian-Albrechts-Universität zu Kiel, Fed. Rep. of Germany

Z. Naturforsch. **49a**, 490–496 (1994); received November 27, 1993

We present the set-up of a molecular beam Fourier transform microwave spectrometer in the range from 26.6 to 40 GHz. As a test we investigated the deuterium hyperfine structure of deutero-acetonitrile, DCH_2CN. It is also shown, that the spectrometer can be used to measure highly resolved rotational spectra of van der Waals complexes.

Introduction

Our pulsed molecular beam (MB) Fourier transform microwave (FTMW) spectrometer for the range from 3 to 26.5 GHz [1, 2] and its modified version for air pollution measurements [3] are very sensitive and accurate tools for the assignment of rotational spectra of molecules and van der Waals complexes and some of their isotopomeres in natural abundance. This encouraged us to add another spectrometer for the range from 26.5 to 40 GHz. The enlarged range helps to exploit the information contained in rotational spectra which extend over the microwave and millimeter wave region.

We give tests of the spectrometer with carbonylsulfide, OCS, and two van der Waals complexes and report, as an example, the investigation of the D- and ^{14}N-hyperfine structure in the rotational spectrum of methylcyanide-d_1. The measurements in the range of the spectrometer proved to be essential.

Set Up

The first MB-FTMW spectrometer has been described by Balle and Flygare [4]. Our set up is given in Figure 1. Since in the region from 26.5 to 40 GHz some MW components are not available and/or very expensive, the polarizing frequency v_p is produced by frequency doubling.

Reprint requests to Prof. Dr. H. Dreizler, Institut für Physikalische Chemie, Universität Kiel, Olshausenstr. 40–60, D-24098 Kiel, Fed. Rep. of Germany.

The synthesizer **1** produces frequencies v_s up to 20 GHz in 1 kHz steps with a power level of up to +20 dBm. It is referenced to the DCF 77 (Mainflingen) standard frequency by the receiver **34**, quartz oscillator **35**, and the frequency multiplier **36**. Via the power divider **2** the power is guided into the polarization and superheterodyne detection branches.

The single sideband modulator **5** produces a frequency of $\frac{1}{2}\, v_p = v_{s\,(-)}^{+}\, 160$ MHz and suppresses the carrier by 15 dB in a sequence determined by the single pole double throw (SPDT)-PIN switch **6**. Thereby polarizing pulses are formed. After amplification **7** the frequency is doubled **8** and again amplified **9**. The power meter **11** connected to the directional coupler **10** allows, together with the attenuators **3** and **4**, an automatic adjustment of the power. This adjustment is made under continuous wave condition and kept constant when pulses are produced. The SPDT PIN switch **12**, one output terminated **13**, helps in pulse formation and increases isolation during the detection period, as a leakage to the detection branch should be minimized to avoid perturbing signals. The PIN switch **14** guides the polarizing pulses into the Fabry-Perot cavity **15** by the antenna **16**. The antenna **18**, detector **19**, and oscilloscope **20** are used for the adjustment of the cavity **15** with the encoder mike **21**. The A/D converter **22** is necessary for automatic broadband scanning.

The transient emission produced in the cavity is directed to the detection system with the PIN switch **14**. Properly synchronized a supersonic molecular beam is produced with the nozzle **17**.

After preamplification **23** the transient signal is down-converted to a band around 320 MHz. The local power of frequency v_s is adjusted with **1** under

0932-0784 / 94 / 0300-0490 $ 01.30/0. – Please order a reprint rather than making your own copy.

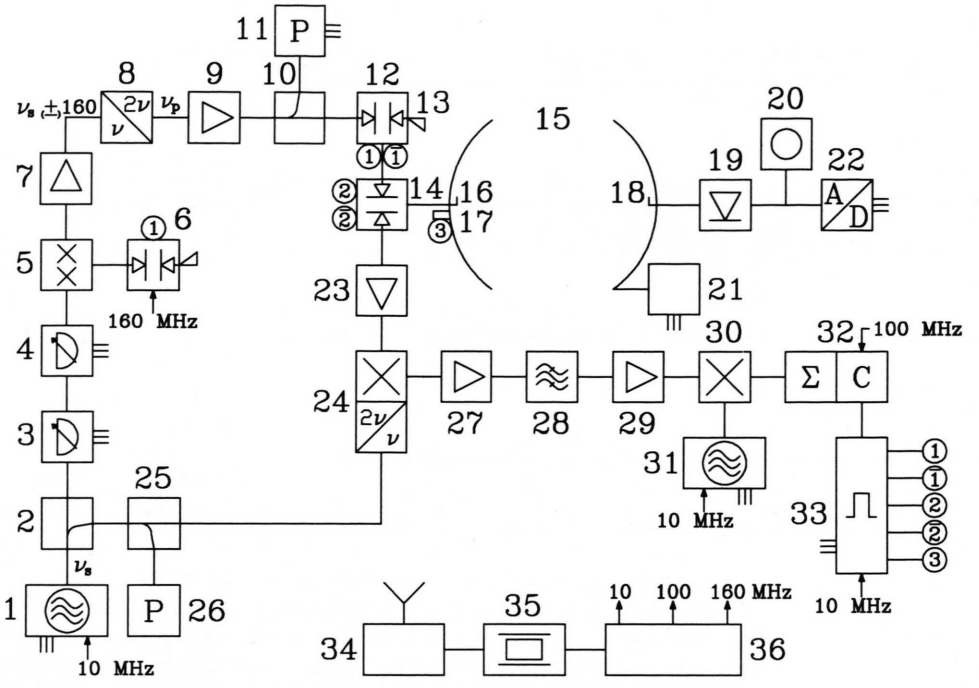

Fig. 1. Set up of the molecular beam Fourier transform microwave spectrometer 26.5–40 GHz. **1.** Microwave synthesizer, Hewlett-Packard (HP), 83 624 A, 2–20 GHz, 1 kHz step width, output + 20 dBm. — **2.** Power divider, M/A-Com, PN 20810-6202-00, 8–26.5 GHz. — **3.** Programmable step attenuator, HP 84907 L, DC-40 GHz, 70 dB, 10 dB steps. — **4.** Programmable step attenuator, HP 84904 K, DC-26.5 GHz, 11 dB, 1 dB steps. — **5.** Single sideband modulator, Watkins-Johnson, M34C-4, carrier and unwanted sideband suppression 22 dB typ. conversion loss 7.5 dB typ. — **6.** SPDT PIN switch, Mini Circuits, ZYSW-2-50 DR. — **7.** Microwave amplifier, HP 8349 B, 2–20 GHz, gain > 13–15 dB, output 18–20 dBm, noise figure < 13 dB. — **8.** Millimeter source module, doubler to 26.5–40 GHz, HP 83554 A. — **9.** Millimeterwave amplifier, HP 8346 A, 26.5–40 GHz, gain > 8–10 dB, output > + 13–+ 17 dBm, noise figure < 13 dB. — **10.** Directional coupler, Krytar, 10–40 GHz, 10 dB. — **11.** Power meter and sensor, HP 437 B, HP 8487 A, 0.05–50 GHz. — **12.** SPDT PIN switch, General Microwave, F 9023, 18–40 GHz, isolation 55 dB, insertion loss max. 4.5 dB. — **13.** Termination, DC-40 GHz. — **14.** SPDT PIN switch, General Microwave. F 9022, 18–40 GHz, isolation 40 dB, insertion loss 4 dB max. — **15.** Fabry Perot cavity, mirror diameter 250 mm, radius of curvature 550 mm, quality factor $Q = 30\,000$. — **16.** Antenna. — **17.** Pulsed molecular beam nozzle with driver, General Valve, Ser. 9 (modified) and IOTA one. — **18.** Antenna. — **19.** Detector diode, HP 8474 D, 0.01–40 GHz. — **20.** Oscilloscope. – **21.** Encoder mike and controller, Oriel 18266 and 18011. — **22.** Analog to digital converter. — **23.** Millimeter wave amplifier, waveguide with coax transitions Hughes A 1350 H-3001, 26.5–33 GHz, gain 21 dB, NF = 5.5 dB Hughes A 1355 H-3601, 33–40 GHz, gain 17 dB, NF = 6 dB. — **24.** 2nd Harmonic Mixer, Pacific Millimeter Products, KaM, 26.5–40 GHz. — **25.** Directional coupler, HP 87300 B, 10 dB, 1–20 GHz. — **26.** Power meter and sensor HP 435 B, HP 8485 A, 0.05–26.5 GHz. — **27.** IF-amplifier, Trontech W 500 H, 5–500 MHz, gain 20 dB, NF = 1.8 dB. — **28.** Bandpass filter, Reactel 4 BE-320-2 522, 320 MHz, bandwidth 2 MHz. — **29.** IF-amplifier, Avantek, GPD 461, 462, 464. — **30.** IF Mixer, Mini Circuits, ZAD1-WH. — **31.** Signal Generator, HP 8656 B, 0.1–990 MHz, 10 Hz steps, + 13 dBm. — **32.** Transient recorder and 486 computer Dr. Strauss Elektronik. TR-AS 100-8, 8 bit, minimum sample interval 10 ns, 32 K record length. — **33.** Synchronized pulse generator (home made). — **34.** Normal frequency receiver, Rohde & Schwarz, XKE 2. — **35.** Regulated quartz oscillator, Rohde & Schwarz, XSD 2. — **36.** Frequency multiplier (home made) to 10, 100, and 160 MHz.

control of the power meter **26** via the directional coupler **25**.

As usual in similar systems, the down converted transient signal is amplified **27**, **29**, and filtered **28**. With the signal generator **31** and mixer **30** the signal is down converted a second time to a frequency band depending on the local frequency. This is usually chosen to be 317.5 MHz, yielding a second intermediate frequency of 2.5 MHz.

The transient signal is digitized in the transient recorder **32** combined with a personal computer for averaging and experiment control. The necessary pulse sequences are produced with the pulse generator **33** under program control by **32**. The sequences are given in Figure 2.

In Fig. 2 the timing diagram for the production of MW pulses by the switches **6**, **12** and **14** is given. In addition the period of the connection of the polariza-

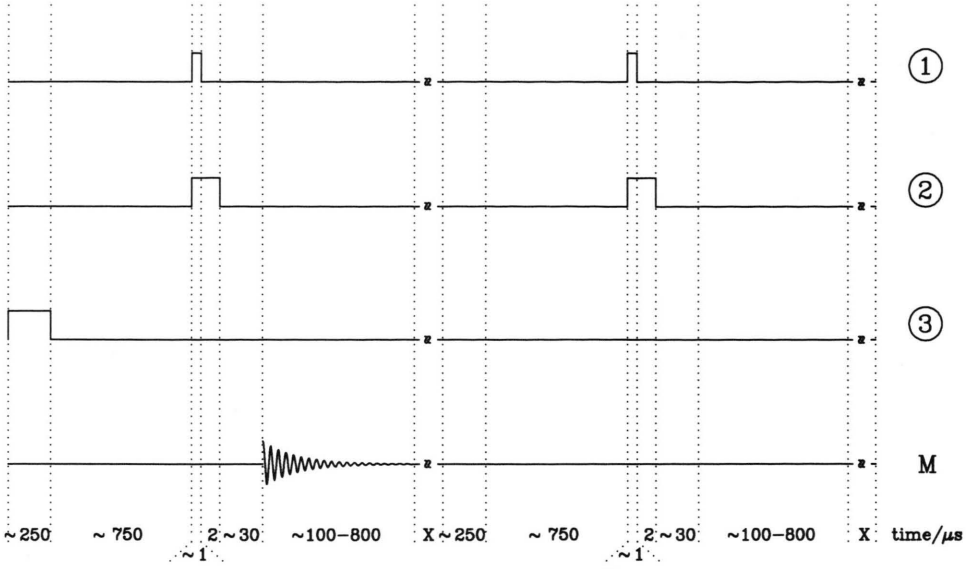

Fig. 2. Timing diagram of MW and molecular beam pulses. ①: TTL-Signal of PIN-switches **6** and **12** of Fig. 1; logic high, left port of **6** and port ① of **12** are open. ②: TTL-Signal of PIN-switch **14** of Fig. 1; logic high, port ② is open. The TTL signals ① and ② are logically inverted with respect to ① and ②. When TTL-signals ① and ② are high, the polarisation branch is connected to the resonator. When ② is high, the resonator is connected to the detection branch. ③: Signal logic high: beam nozzle is open. M: molecular response signal. The measurement without a molecular beam is used to compensate the influence of the MW system. X is a delay which determines the repetition rate of the experiment cycles. Not to scale.

tion branch **3–12** to the cavity **15** and the period of the connection to the detection branch **23–29** is displayed together with the period of measurement **M**.

In Fig. 3 we give a drawing of the mechanical construction of the cavity. The quality factor is $Q = 30\,000$.

One mirror **1** of the cavity is placed inside a planar flange **2** of the vacuum tank **3**. The nozzle **4** is mounted near the center of the mirror (distance 25 mm), the antenna **5** in the center of the mirror. The MW is introduced by a vacuum tight connector **6** on which the antenna **5** is positioned. The second mirror is arranged in a way that the cylinder symmetry of the cavity is maintained under adjustment of the cavity length.

The second mirror **7** is fixed on a ball bearing carriage **8** moving on two cylindrical precision axes of 12 mm diameter with a maximum displacement of 37 mm. The carriage **8** is mounted between two rings **9**. The rings are held parallel by two rods **10**. This mirror unit is mounted on the flange **2** by four rods **11**. The rods **10**, **11**, and rings **9** are manufactured from PVC to reduce reflections of microwave radiation. Using an encoder mike **12** the mirror is adjusted for resonance of the cavity. The mirror is drawn back by two springs.

The described construction is the most simple arrangement we tested. Only some dimensions of the parts (mirror surface, thickness of the rings, length of the rods) must be manufactored precisely.

Test of Performance

As usual in MW spectroscopy, carbonyl sulfide, OCS, and its isotopomeres were used as test molecules.

In Fig. 4 the transition $J = 3$–2 of $^{18}O^{13}CS$ recorded in 1300 s with an experiment repetition rate of 5 Hz is shown. At room temperature this transition would have an absorption coefficient of $\alpha = 4 \cdot 10^{-9}\ cm^{-1}$. It should be noticed that the absorption coefficient is not a correct measure for sensitivity for this type of spectroscopy. It is given just for comparison with MW Stark spectroscopy. It should also be mentioned that with a waveguide FTMW spectrometer we reached a higher sensitivity as shown in Fig. 3 of [5].

The line width is demonstrated in Fig. 5 for the $J = 3$–2 transition of ^{18}OCS in natural abundance.

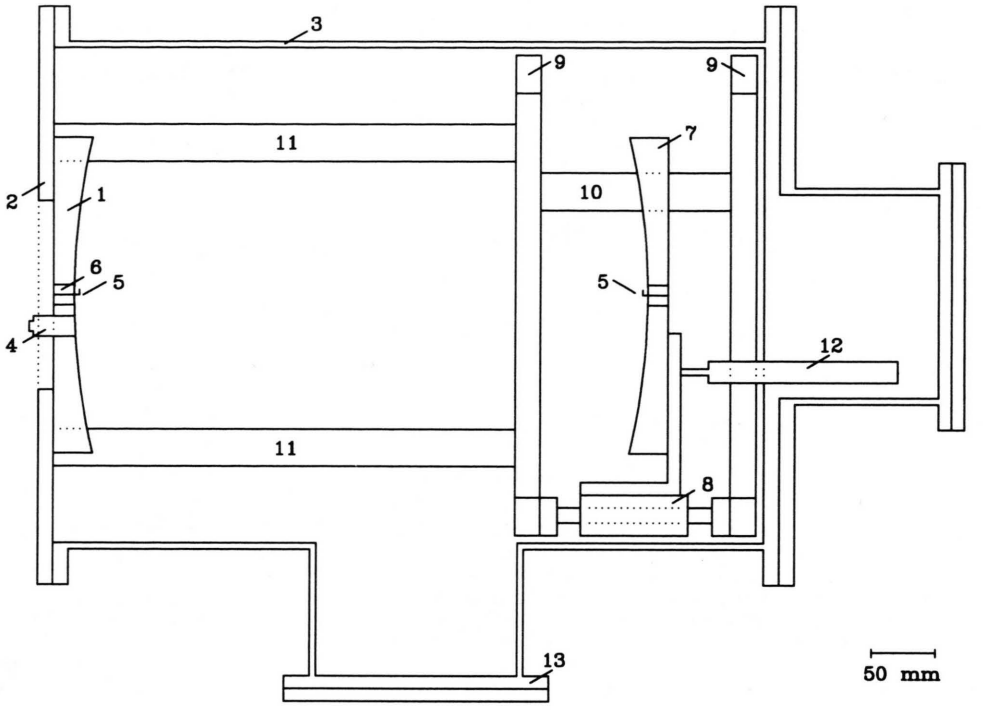

Fig. 3. Mechanical construction of the spectrometer. **1.** Mirror, aluminium AlMgSil, diameter 250 mm, radius of curvature 550 mm. — **2.** Planar flange of the vacuum tank, diameter 458 mm with a central hole of diameter 150 mm for access to nozzle **4** and MW connector **6**. — **3.** Vacuum tank, stainless steel, inner diameter 392 mm, length 560 mm, wall thickness 5 mm with flange for diffusion pump 1000 l/s (too low pumping rate). — **4.** Nozzle, General valve Series **9**. – **5.** Antenna, mounted on the tip of **6**. — **6.** Vacuum tight connector, Omni-Spectra, M/A-Com OS-50 (2.4) female, metal to metal seal P.N. 8558-5219-000 with adapter to OS 2.9 mounted in a special insert in the mirror center. — **7.** Mirror, dimension see **1**. — **8.** Ball bearing carriage with stainless steel axes length 150 mm, maximum displacement 37 mm, Star, part number 1040-712-30. — **9.** Ring, PVC, inner/outer diameter 320/386 mm, thickness 20 mm. — **10.** 2 Rods, PVC, length 150 mm, diameter 30 mm. — **11.** 4 Rods, PVC, length 360 mm, diameter 30 mm. — **12.** Encoder mike, Oriel 18011 and 18266. 50 mm maximum displacement. — **13.** Flange DN 160 JSO KF for vacuum pump.

Here we obtained a half width at half height (HWHH) of 2.8 kHz. For the $J = 1-0$ transition we obtained with the MB-FTMW spectrometer for the 3 to 26 GHz region [2] a HWHH of 1 kHz at 11.8 GHz. In the present case the transit time with 0.96 ms contributes with $\Delta\nu_T = 1$ kHz more to the linewidth than the transit time of 1.5 ms and $\Delta\nu_T = 0.7$ kHz does for the $J = 1-0$ transition. If one speculates that the linewidth is predominantly determined by a Doppler broadening due to velocity inhomogeneities of the beam, the line width should increase by a factor 3 for lines near 34.2 GHz compared to lines near 11.8 GHz. It should be stated that a precise understanding of the contributions to the linewidth for the experimental situation is presently not available.

In Fig. 6 and Fig. 7 we present recordings of spectra of van der Waals complexes. As the low beam temperatures favor the production of van der Waals complexes, the beam spectrometers also provide a tool for these species. In Fig. 6 a spectrum of the $OC^{34}S$–Ar complex: $J_{K-K+} = 3_{31}-2_{21}$ is presented. Figure 7 shows a spectrum $J_{K-K+} = 5_{05}-4_{04}$ of the NH_3-CO_2 van der Waals complex.

Deuteroacetonitrile, DCH_2CN

Acetonitrile is very abundant in interstellar space. Because of its high dipole moment the rotational spectrum is strong and is used as a probe of temperature and density of molecular clouds. Because of its intense spectrum it seems possible that the monodeuterated species could also be detected.

The ground state rotational spectra of DCH_2CN (main, ^{13}C, and ^{15}N isotopomeres) were investigated

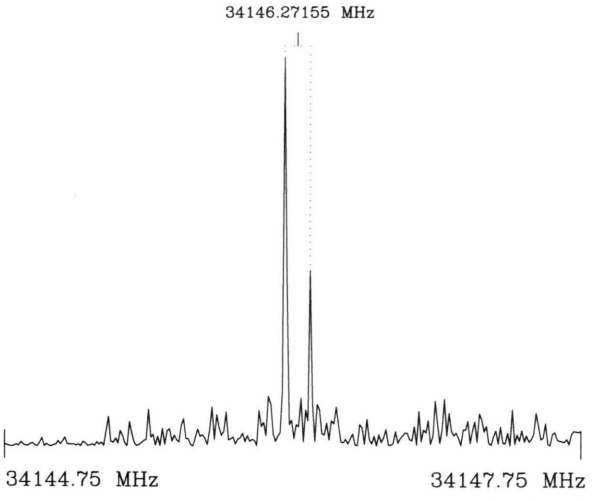

Fig. 4. Power spectrum of the transition $J = 3-2$ of carbonyl sulfide, $^{18}O^{13}CS$, in natural abundance at 34146.2715 MHz. 1% OCS in argon. Absorption coefficient $\alpha = 4 \cdot 10^{-9}$ cm^{-1}. 40 ns sample interval, 8 k data points, 6528 experiment cycles, 1300 s measuring time, 34146.25 MHz polarizing frequence, 12 mW power, 0.5 μs MW pulse width, 30 μs measurement delay, 50 kPa backing pressure.

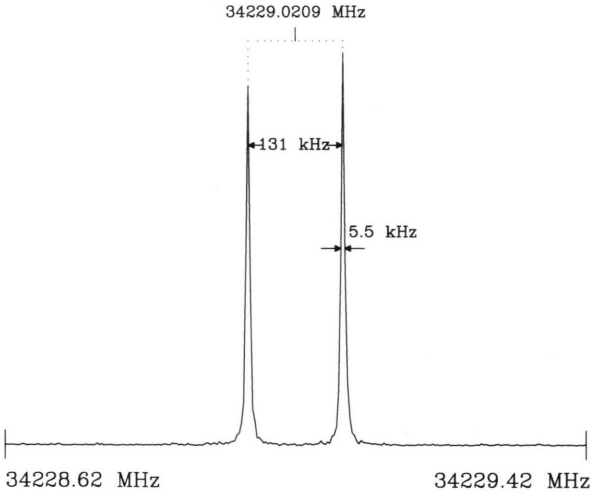

Fig. 5. Power spectrum of the transition $J = 3-2$ of carbonyl sulfide, ^{18}OCS in natural abundance at 34229.0209 MHz. 1% OCS in argon. Line width (HWHH) $\Delta\nu = 2.8$ kHz. 50 experiment cycles, 10 s measuring time, 34229.02 MHz, polarizing frequency. Other experiment parameters see Fig. 4.

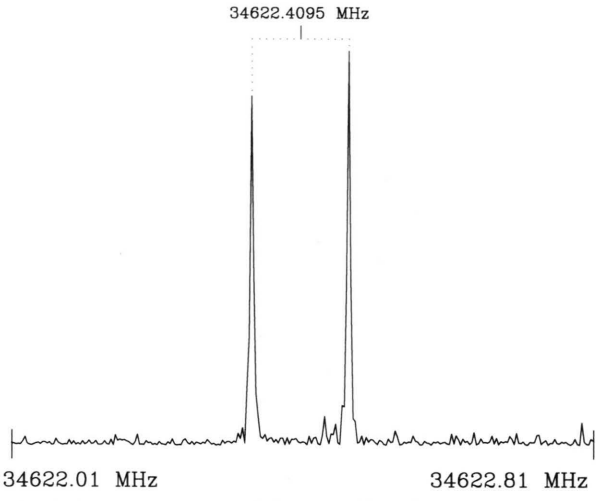

Fig. 6. Power spectrum of the transition $J_{K-K+} = 3_{31}-2_{20}$ of the van der Waals complex $OC^{34}S$-Ar in natural abundance at 34622.4095 MHz. 1% OCS in argon. 40 ns sample interval, 8 k data points, 1384 experiment cycles, 277 s measuring time, 1 mW 34622.41 MHz, polarizing frequency, 1 mW MW power, 0.8 μs MW pulse width, 30 μs measuring delay, 50 kPa backing pressure.

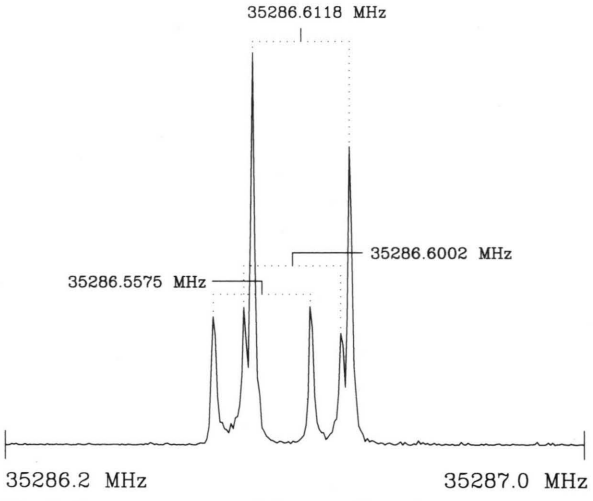

Fig. 7. Power spectrum of the transition $J_{K-K+} = 5_{05}-4_{04}$ of the van der Waals complex NH_3–CO_2 near 35286.6118 MHz showing ^{14}N-hfs. 0.5% NH_3, 2.5% CO_2 in argon. 40 ns sample interval, 8 K data points, 120 experiment cycles, 24 s measuring time, 35286.60 MHz polarizing frequency, 5 mW MW power, 0.5 μs MW pulse width, 30 μs measurement delay, 100 kPa backing pressure.

recently by Le Guennec et al. [6]. The authors determined rotational and centrifugal distortion constants and an equilibrium structure.

Because DCH_2CN is a light near symmetric top molecule, the low J-transitions, which contain an important information on the quadrupole coupling constants, occur at relatively high frequencies ($J'-J$: 2–1 at 35 GHz). Because of the smallness of the D and ^{14}N coupling effects, which were within the Doppler broadening under static gas conditions, the coupling

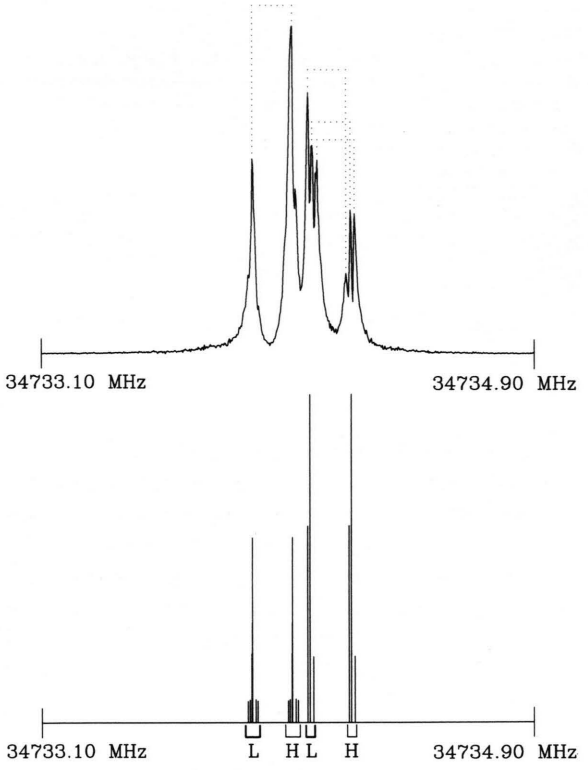

Fig. 8. DCH_2CN. a) Power spectrum of the lower frequency part of the transition $J_{K-K+} = 2_{02}-1_{01}$. It should be noted that lines separated by only 7 kHz (s. Table 1) could be resolved even at frequencies around 35 GHz. 1% substance in argon. 40 ns sample interval, 8 K datapoints, 110 experiment cycles, 22 s measuring time, 34734.1 MHz polarizing frequency, approx. 10 mW power, 1 μs MW-pulse width, 30 μs measurement delay approx. 50 kPa backing pressure. b) Theoretical spectrum, Doppler components H shifted to higher frequencies, components L to lower frequencies.

constants could not be determined by conventional microwave spectroscopy. With the Q-band beam spectrometer we were able to determine the quadrupole coupling constants. MB-FTMW spectroscopy provides sufficient resolution even in this frequency region.

Experimental

Using the apparatus described above we recorded the a-type $J = 2-1$ transitions of DCH_2CN in the 35 GHz range. Additionally we also measured the $J_{K-K+} = 1_{01}-0_{00}$ transition with our MB-FTMW spectrometer [1, 2] in the 17 GHz region. The DCH_2CN sample was kindly provided by J. Demaison, Lille. It was used without further purification as a 1% mixture in argon at a stagnation pressure of about 100 kPa.

Analysis

The observed rotational transitions of DCH_2CN were split due to nitrogen-14 and deuterium quadrupole hyperfine coupling. An example is given in Figure 8. For the analysis of the hyperfine structure a first order calculation in the $I_1 + I_2 = I$, $I + J = F$ coupling scheme was used. This coupling scheme is not really adequate for very differently coupling nuclei. So the intermediate quantum number I should be regarded more as a label than a physically significant quantum number. The hyperfine components as well as the hyperfine free line centers are given in Table 1. The results of a fit are summarized in Table 2. It should be pointed out that the deuterium coupling constants could be obtained only because of the high resolution in the 35 GHz region.

Discussion

For comparison with other molecules it is useful to calculate the coupling constants in coordinates, where one of them is aligned with the respective bond axis and, assuming a cylindrical symmetry, the others are perpendicular to it. For the C–N as well as the C–D bond this transformation corresponds to a rotation around the c-axis. Therefore χ_{cc} is not affected by the rotation and is defined to be χ_{yy}. Since the coupling tensor is traceless, and due to a cylindrical symmetry around the bond axis $\chi_{xx} = \chi_{yy}$, one obtains $\chi_{zz} = -2\chi_{xx} = -2\chi_{cc}$ without reference to the structure.

Using the data given in Table 2 yields $\chi_{zz}(^{14}N) = -4.2166(58)$ MHz and $\chi_{zz}(D) = 0.191(11)$ MHz. This value is in good agreement with theoretical calculatons of Huber [7] resulting in $\chi_{zz}(D) = 0.1741$. The author also predicted 4.3% asymmetry of the C–D bond for methylcyanide, which justifies the assumption that the tensor is cylindrical symmetric. Comparing the results with the experimental data of CH_3CN: $\chi_{zz}(^{14}N) = -4.224(4)$ MHz [8] and of CD_3CN: $\chi_{zz}(^{14}N) = -4.2292(6)$ MHz and $\chi_{zz}(D) = 0.1696(45)$ MHz [9] we also find a good agreement. The $\chi_{zz}(D)$ [9]

Table 1. Rotational transitions of deuteroacetonitrile. v: measured frequency/MHz, $\Delta v = v_0 - v$: observed quadrupole splitting/MHz, δ_{hfs}: difference between observed and calculated frequency of the hyperfine component/kHz. v_0: hypothetical unsplit line frequency/MHz.

$J'_{K'-K'+} - J_{K-K+}$	F' I' $-$ F I	v	Δv	δ_{hfs}	v_0
$1_{0\ 1} - 0_{0\ 0}$	1 2 − 2 2	17369.833	2.107	−2	17367.726(1)
	1 1 − 0 0	17367.949	0.223	2	
	3 2 − 2 2	17367.940	0.214	1	
	2 1 − 1 1	17367.931	0.205	4	
	1 0 − 2 2	17366.675	−1.051	−3	
	2 2 − 2 2	17366.669	−1.057	−1	
	0 1 − 1 1	17366.657	−1.069	0	
$2_{1\ 2} - 1_{1\ 1}$	1 2 − 1 2	34585.738	1.596	0	34584.142(1)
	2 0 − 1 2	34585.722	1.580	−1	
	0 2 − 1 2	34585.703	1.560	1	
	2 1 − 1 1	34584.417	0.275	6	
	4 2 − 3 2	34584.399	0.257	0	
	3 1 − 2 1	34584.391	0.249	−2	
	1 2 − 2 2	34584.151	0.009	1	
	2 0 − 2 2	34584.132	−0.010	−3	
	1 2 − 0 1	34584.113	−0.029	−3	
	1 1 − 1 1	34583.735	−0.407	−1	
	3 2 − 3 2	34583.719	−0.423	−6	
	2 2 − 2 1	34583.713	−0.429	7	
	2 2 − 1 0	34583.116	−1.026	1	
	2 2 − 2 2	34583.094	−1.048	−1	
	3 2 − 2 2	34583.079	−1.063	−0	
	1 1 − 0 1	34583.039	−1.104	1	
$2_{1\ 1} - 1_{1\ 0}$	0 2 − 1 2	34887.066	1.619	−1	34885.447(1)
	2 0 − 1 2	34887.031	1.584	−3	
	1 2 − 1 2	34887.013	1.566	1	
	2 1 − 2 1	34885.748	0.301	1	
	4 2 − 3 2	34885.716	0.269	7	
	3 1 − 2 1	34885.695	0.248	7	
	2 0 − 2 2	34885.450	0.003	−4	
	2 0 − 1 0	34885.435	−0.013	−4	
	3 2 − 3 2	34885.024	−0.423	−2	
	1 1 − 0 1	34884.433	−1.015	−2	
	3 2 − 2 2	34844.400	−1.047	0	
	2 2 − 1 0	34884.358	−1.090	−2	
$2_{0\ 2} - 1_{0\ 1}$	2 0 − 2 2	34737.334	2.118	6	34735.216(1)
	2 0 − 2 2	34737.314	2.099	−5	
	2 0 − 3 2	34736.054	0.838	−4	
	0 2 − 1 2	34734.175	−1.040	0	
	2 0 − 1 2	34734.168	−1.047	6	
	1 2 − 1 2	34734.152	−1.064	−3	
	3 2 − 3 2	34733.949	−1.267	−1	

of CD_3CN was also obtained with the assumption of a cylindrical bond but using the 1–0 transition and the molecular structure.

Table 2. ^{14}N- and D-Quadrupole Coupling Constants of DCH_2CN. Fitparameter: $\chi_{aa}(^{14}N)$, $\chi_{bb}(^{14}N)$, $\chi_{aa}(D)$, $\chi_{bb}(D)$ and v_0 the hypothetical unsplit line center. Rotational constants were fixed at the values given in [6]. Standard errors are given in units of the least significant digit. N is the number of all fitted hyperfine components. σ is the standard deviation of the lines in the fit.

$\chi_{aa}(^{14}N)$	−4.2183(23) MHz	$\chi_{cc}(^{14}N)$	−2.1083(29) MHz
$\chi_{bb}(^{14}N)$	2.1100(30) MHz	$\chi_{cc}(D)$	0.0954(52) MHz
$\chi_{aa}(D)$	−0.0562(54) MHz	$\chi_{zz}(^{14}N)$	−4.2166(58) MHz
$\chi_{bb}(D)$	0.1516(51) MHz	$\chi_{zz}(D)$	0.191(11) MHz
N	42		
σ	3.8 kHz		

Because our coupling constants in bond axes were achieved independently of structural informations they may be used to confirm the molecular structure. Therefore the rotation angles α between the a-axis and the bond axes were calculated from the r_s-structure reported in [6]. For the C–N axis, α was found to be 1.795°, for the C–D axis α is 68.102°. Using the well known transformation [10]

$$\chi_{aa} = \chi_{xx} \sin^2 \alpha + \chi_{zz} \cos^2 \alpha,$$

$$\chi_{bb} = \chi_{xx} \cos^2 \alpha + \chi_{zz} \sin^2 \alpha$$

one obtains $\chi_{aa}(^{14}N) = -4.210$ MHz, $\chi_{bb}(^{14}N) = 2.110$ MHz, $\chi_{aa}(D) = -0.0561$ MHz, $\chi_{bb}(D) = 0.1515$ MHz which is in good agreement with the experimental results and confirms the r_s-structure of the molecule.

Acknowledgements

We thank the members of our group especially Dr. J.-U. Grabow and Dr. N. Heineking for help and discussions. Without the valuable help of our mechanic workshop under Mr. K.-D. Will the spectrometer would never have come to a successful operation. We further thank Prof. Dr. J. Demaison for providing the DCH_2CN sample. Our work was funded by the Deutsche Forschungsgemeinschaft, the Fonds der Chemie and the Land Schleswig-Holstein.

[1] U. Andresen, H. Dreizler, J.-U. Grabow, and W. Stahl, Rev. Sci. Instrum. **61,** 3694 (1990).
[2] J. U. Grabow and W. Stahl, Z. Naturforsch. **45a,** 1043 (1990).
[3] U. Andresen, H. Dreizler, U. Kretschmer, W. Stahl, and C. Thomsen, Fresenius' Z. Anal. Chem. to be published.
[4] T. J. Balle and W. H. Flygare, Rev. Sci. Instrum. **52,** 33 (1981).
[5] Ch. Keussen, R. Schwarz, U. Andresen, and H. Dreizler, Z. Naturforsch. **45a,** 711 (1990).
[6] M. Le Guennec, G. Wlodarczak, J. Burie, and J. Demaison, J. Mol. Spectrosc. **154,** 305 (1992).
[7] H. Huber, J. Chem. Phys. **83,** 4591 (1985).
[8] S. G. Kukolich, J. Chem. Phys. **76,** 97 (1982).
[9] A. M. Murray and S. G. Kukolich, J. Chem. Phys. **78,** 3557 (1983).
[10] W. Gordy and R. L. Cook, Microwave Molecular Spectra, John Wiley & Sons, New York 1984, 3rd edition, p. 419, eq. 9.115, 9.116.